Torque Ripple Minimization of High-Power Fed Induction Motor Drive Using Low Switching Frequency

G. Durga sukumar,M. K. Pathak*
Electrical Engineering Department, IIT Roorkee, India-247667

ABSTRACT

Multi-level inverter has emerged as an important topology in the area of high-power-medium voltage energy control applications due to its several advantages such as its good harmonic rejection capability, better output voltage with reduced ripple, reduction of voltage ratings of the power semiconductor switching devices and also the reduced electro-magnetic interference problems, etc. This paper presents the torque ripple minimization and the performance under different operating conditions (dynamic and steady state) of indirect vector-controlled high-power fed induction motor driven by three-level inverter with the low switching frequency 0.51 kHz. It also presents simplified space-vector modulation method for a three-level inverter. The torque ripple of induction motor drive fed with a two-level inverter and a three-level inverter is compared. The total harmonic distortion values of inverter line-to-line voltages and induction motor phase current values are also compared using two-level inverter and three-level inverter.

***Keywords**: Multi-level inverter, performance improvement, THD reduction, two-level inverter, space-vector modulation (SVM), indirect vector control*

****Author for Correspondence*** Email: durgadee@iitr.ernet.in

INTRODUCTION

Vector control is used in induction motor drives for high dynamic and better performance [1,2]. This performance can be improved by using multi-level inverter instead of two-level inverter. In a conventional two-level inverter, the harmonic reduction of an inverter output is achieved mainly by raising the switching frequency. But in high-power applications, the switching frequency of the power device is restricted to 1 kHz due to the increased switching losses and also the level of dc-bus voltage. So from the aspect of harmonic reduction and better output, voltage multi-level inverter is used instead of a two-level inverter.

An indirect vector control of induction motor drive control is presented [3]. In this, it uses hysteresis current and torque controllers to control the stator currents in order to obtain better performance. A PI and fuzzy logic-based speed controller in indirect vector-controlled induction motor drive are compared [4]. In this, a fuzzy logic controller gives better dynamic and steady state performance compared to a PI controller. A genetic algorithm-particle swarm optimization-based indirect vector control for optimal torque control of induction motor has been presented [5]. In all the above methods, techniques to decrease torque ripple optimization are used. An adaptive robust control for induction motor drives based on the sliding mode control theory is presented [6]. It is noted that all the above vector-control methods use two-level inverter and use optimization techniques with relatively high-switching frequency above 10 kHz but cannot accomplish satisfactory

torque ripple reduction. In order to implement optimization technique, one should have better knowledge. This problem can be solved using multi-level inverters in the vector control. However, regardless of its advantages, vector control with multi-level inverters with low switching frequency < = 1 kHz is still mostly unexplored.

The concept of the multi-level pulse width modulation (PWM) converter and various modulation strategies have been developed and studied [7–13]. In all these strategies, space-vector modulation (SVM) stands out because it offers significant flexibility to optimize switching waveforms and it is well suited for implementation on a digital computer. A new simplified space-vector pulse-width modulation (SVPWM) method for three-level inverter is proposed [14]. A relationship between space-vector modulation and carrier-based pulse-width modulation for multi-level inverter has been presented [15].

In this paper, an indirect vector control scheme with two- and three-level inverter-fed induction motor drive operating with low switching frequency of 1 kHz and the performance and torque ripple of induction motor at different operating conditions is compared. In this, Modeling of induction motor and indirect vector control is introduced in the second section. The third section contains space-vector modulation techniques of two-level and three-level inverters. Block diagram of the proposed vector control and simulation results of 3-Phase, 100 hp, 400 V, 50 Hz, and 1460 RPM induction machine are presented in the fourth section. Finally, concluding remarks are stated in the fifth section. The parameters of motor are given in Appendix.

MODELLING OF INDUCTION MOTOR AND INDIRECT VECTOR CONTROL

The mathematical model and torque of a three-phase induction motor in stator reference frame can be expressed as [16]

$$V_{qs} = R_s i_{qs} + p\lambda_{qs} \quad (1)$$
$$V_{ds} = R_s i_{ds} + p\lambda_{ds} \quad (2)$$
$$0 = R_r i_{qr} + (-\omega_r)\lambda_{dr} + p\lambda_{qr} \quad (3)$$
$$0 = R_r i_{dr} - (-\omega_r)\lambda_{qr} + p\lambda_{dr} \quad (4)$$

where (i) V_{ds}, V_{qs} and V_{dr}, V_{qr} are d-q axis stator and rotor voltages respectively

(ii) i_{ds}, i_{qs} and i_{dr}, i_{qr} are d-q axis stator and rotor currents respectively

(iii) R_s and R_r are stator and rotor resistances per phase respectively

(iv) λ_{qs}, λ_{ds} and λ_{qr}, λ_{dr} are stator and rotor flux linkages respectively

(v) ω_r is rotor angular speed

Stator and Rotor flux linkages can be given as

$$\lambda_{qs} = L_s i_{qs} + L_m i_{qr} \quad (5)$$
$$\lambda_{ds} = L_s i_{ds} + L_m i_{dr} \quad (6)$$
$$\lambda_{qr} = L_r i_{qr} + L_m i_{qs} \quad (7)$$
$$\lambda_{dr} = L_r i_{dr} + L_m i_{ds} \quad (8)$$

where *Ls, Lr* are self inductances of stator and rotor respectively and *Lm* is mutual inductance.

From the above equations (1)(8), a squirrel-cage induction motor can be described in stator reference frame as

$$\begin{bmatrix} V_{qs} \\ V_{ds} \\ 0 \\ 0 \end{bmatrix} = \begin{bmatrix} R_s + pL_s & 0 & pL_m & 0 \\ 0 & R_s + pL_s & 0 & pL_m \\ pL_m & -\omega_r L_m & R_r + pL_r & -\omega_r L_r \\ \omega_r L_m & pL_m & \omega_r L_r & R_r + pL_r \end{bmatrix} \begin{bmatrix} i_{qs} \\ i_{ds} \\ i_{qr} \\ i_{dr} \end{bmatrix} \quad (9)$$

where $\omega_r = \frac{d\theta}{dt}$ and $p = \frac{d}{dt}$

The electromagnetic torque *Te* of the induction motor is given by

$$T_e = \frac{3}{2}\left(\frac{P}{2}\right) L_m \left(i_{qs} i_{dr} - i_{ds} i_{qr}\right) \quad (10)$$

In indirect vector control, the rotor flux is aligned along the d-axis then the q-axis rotor flux $\lambda qr = 0$. So from the Eqs. (7) and (10), the electromagnetic torque of the motor can be expressed as

$$T_e = \frac{3}{2}\left(\frac{P}{2}\right) \frac{L_m}{L_r} \lambda_{dr} i_{qs} \quad (11)$$

In indirect vector control, the rotor angle θ is estimated in an indirect manner using the measured rotor speed *ωr* and slip speed *ωsl*

$$\theta = \int \omega_e dt = \int (\omega_r + \omega_{sl}) dt \quad (12)$$

As the rotor flux aligned on d-axis, using Eqs. (3) and (7) leads

$$\omega_{sl} = \frac{L_m R_r}{\lambda_{dr} L_r} i_{qs} \quad (13)$$

From the respective errors of reference values of currents to that of the actual values V_{ds} and V_{qs} are obtained.

SPACE-VECTOR MODULATION (SVM)

Two-Level SVM

Figure 1 represents the two-level inverter circuit and its space-vector diagram with eight different switching states (V_0–V_7). The effective voltage is zero when the vectors V_0 and V_7 are selected. The remaining six voltage vectors can be selected to apply an effective voltage to the machine.

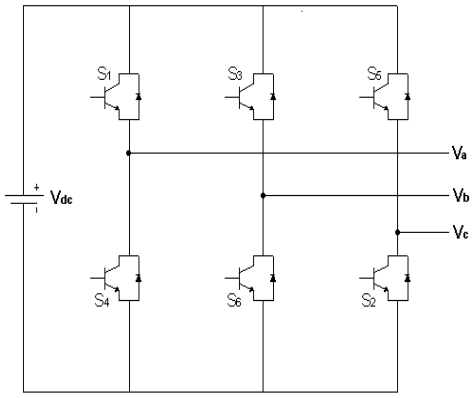

(a)

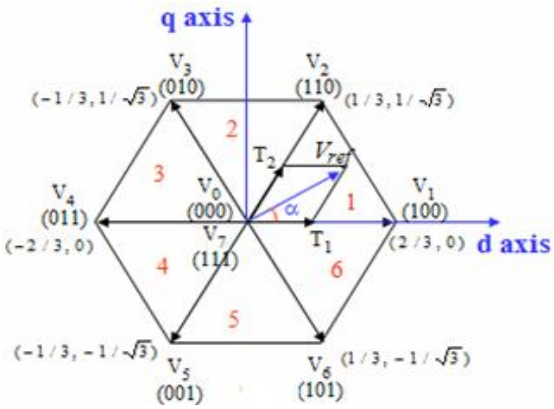

(b)

Fig.1 Two-Level Inverter and Its Space-Vector Diagram with Active Vectors.

A constant reference voltage vector V_{ref} at an angle α can be generated using two zero vectors V_0 and V_7 in combination with two adjacent non-zero vectors V_n and $V_{n+1,}$ From the average voltage concept, the reference vector during one sampling period can be written as

$$V_{ref} = (T_1.V_n + T_2 .V_{n+1})/T_s \quad (14)$$

where T_1, T_2 are the times for which V_n and V_{n+1} act respectively.

Equating the volt-seconds along the d-axis,

$$V_{ref}\cos\alpha . T_s = V_{dc}.T_1 + \left(V_{dc}.\cos\frac{\pi}{3}\right)T_2 \quad (15)$$

Equating the volt-seconds along the q-axis,

$$V_{ref}\sin\alpha . T_s = \left(V_{dc}.\sin\frac{\pi}{3}\right)T_2 \quad (16)$$

where α is the angle of V_{ref} in a 60 ^{o} sector with respect to the beginning of the sector and V_{dc} is the magnitude of each active vector (V_1-V_6).

The effective times can be expressed as

$$T_1 = M.\frac{\sin\left(\frac{\pi}{3}-\alpha\right)}{\sin\left(\frac{\pi}{3}\right)}.T_s \quad (17)$$

$$T_2 = M.\frac{\sin(\alpha)}{\sin\left(\frac{\pi}{3}\right)}.T_s \quad (18)$$

$$T_0 = T_s – T_1 – T_2 \quad (19)$$

where Ts = sampling period, T_0= duration of zero vector and M is the modulation index, given by V_{ref}/V_{dc}. To reduce the ripple, the zero vector time is equally distributed within a sampling period.

In the space-vector diagram, the zero and active vectors do not move in the space, thus they are referred as stationary vectors. On the contrary, the reference vector V_{ref} in Figure 1 rotates in space at an angular velocity

$$\Omega = 2\pi f \quad (20)$$

where f is the fundamental frequency of the inverter output voltage. The angular displacement between V_{ref} and d-axis of the d-q plane can be obtained by

$$\alpha(t) = \int_0^t \omega(t)dt + \alpha(0) \quad (21)$$

For a given magnitude and position, Vref can be synthesized by three nearest stationary vectors. Based on this, switching states of the inverter can be selected and the gate signals for the active switches can be generated. When Vref passes through the sectors one by one, different sets of switches will be turned on or off. As a result, when the Vref rotates one revolution in space, the inverter output voltage varies one cycle over time. The inverter output frequency corresponds to the rotating speed of Vref and output voltage can be adjusted by the magnitude of Vref.

Three-Level SVM

In three-level, the space-vector diagram is composed of six hexagons, which can be reduced into the space-vector diagrams of conventional two-level inverters. The space-vector diagram three-level inverter and its two-level hexagons are shown in Figure 2(a) and (b). The corresponding switching states of a-phase of the inverters are given in Table I.

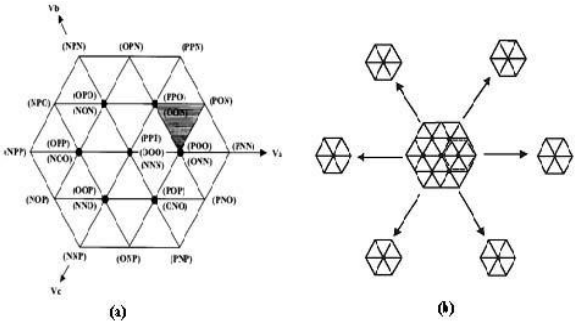

Fig. 2 Space-Vector Diagram of Three-Level Inverter and Six Two-Level Hexagons.

Table I Three-Level Switching States.

Switching symbol	Switching states				Terminal voltage
	S_{1u}	S_{2u}	S_{3u}	S_{4u}	
P	On	On	Off	off	V_{dc}
O	Off	On	On	off	0
N	Off	Off	On	on	$-V_{dc}$

A three-level space-vector plane is transformed to the two-level space-vector plane by using the following two steps:

(1) From the location of a given reference voltage, one hexagon has to be selected.

2) The original reference voltage vector has to be subtracted by the amount of the center voltage vector of the selected hexagon.

If the reference voltage vector is in the regions that are overlapped by adjacent small hexagons, the space-vector diagram can have two values. Once the value is obtained, the origin of a reference voltage vector is changed to the center voltage vector of the selected hexagon by subtracting the center vector of the selected hexagon from the original reference vector. The change of original reference voltage vector (V^*) from three-level to two-level is shown in Figure 3. The difference between the two-level and three-level SVM is multiplying factor 2, which appears in the effective times. The procedure for calculating switching pattern is the same as that of two-level SVM. The effective times are calculated as

$$T_1 = \frac{2.v^{2*}T_s}{v_{dc}.\frac{2}{s}} \cdot \frac{\sin\left(\frac{\pi}{s}-\alpha\right)}{\sin\frac{\pi}{s}} \quad (18)$$

$$T_2 = \frac{2.v^{2*}T_s}{v_{dc}.\frac{2}{s}} \cdot \frac{\sin(\alpha)}{\sin\frac{\pi}{s}}, \quad (19)$$

$$T_0 = T_s T_1 T_2 \quad (20)$$

where $V^{2*}$is the corrected reference voltage of two-level inverter.

Table II gives the d and q components of the reference voltage V^{2*} for all six hexagons after second transformation. After obtaining the corrected reference voltage vector V^{2*} and corresponding hexagons, the conventional two-level space-vector modulation technique is applied as usual.

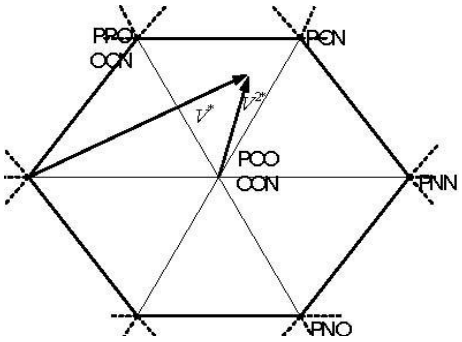

Fig. 3 Change of Original Reference Voltage Vector

Table II d and q Components of the Reference Voltage V^{2*}.

S. No.	V^{2*} d	V^{2*}q
1	$V^{3*}d–2V.\cos(0)$	$V^{3*}d–2V.\sin(0)$
2	$V^{3*}d–2V.\cos(\pi/3)$	$V^{3*}d–2V.\sin(\pi/3)$
3	$V^{3*}d–2V.\cos(2\pi/3)$	$V^{3*}d–2V.\sin(2\pi/3)$
4	$V^{3*}d–2V.\cos(\pi)$	$V^{3*}d–2V.\sin(\pi)$
5	$V^{3*}d–2V.\cos(4\pi/3)$	$V^{3*}d–2V.\sin(4\pi/3)$
6	$V^{3*}d–2V.\cos(5\pi/3)$	$V^{3*}d–2V.\sin(5\pi/3)$

RESULTS AND DISCUSSION

Figure 4 represents the block diagram of indirect vector-controlled high-power fed induction motor drive with two-level and three-level inverters. From the value of reference currents i_{ds}^* and i_{qs}^* to that of actual currents i_{ds} and i_{qs}, d-axis voltage V_{ds} and q-axis voltage V_{qs} is generated using the PI controllers. These voltages are converted into stationary frame and then given to SVM block to generate switching pulses for two- and three-level inverter circuits. The voltage generated from the inverter circuit is given to the induction motor.

The simulation results of indirect vector-controlled high-power induction motor drive fed from two-level and three-level inverters are presented by considering the reference value of speed as 1400 rpm. The sampling frequency taken for the SVM is 1 kHz.

The performance of induction motor drive during the starting is compared in Figure 5(a) and (b). From these figures, the maximum current during the starting is reduced and the ripple content is less with three-level inverter. The torque attains peak value early and the speed response also reaches steady state early with a three-level inverter compared to a two-level inverter.

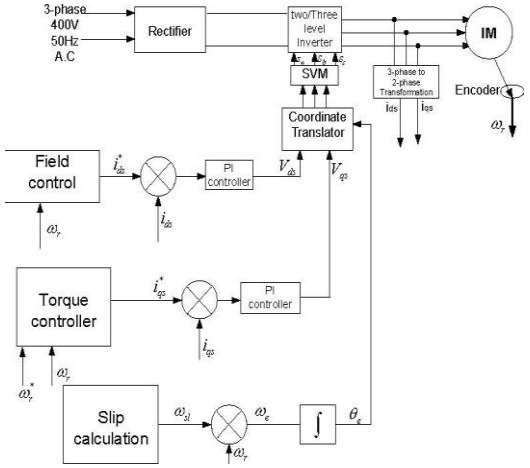

Fig. 4 Proposed Vector Control with Two- and Three-Level Inverter Fed Induction Motor.

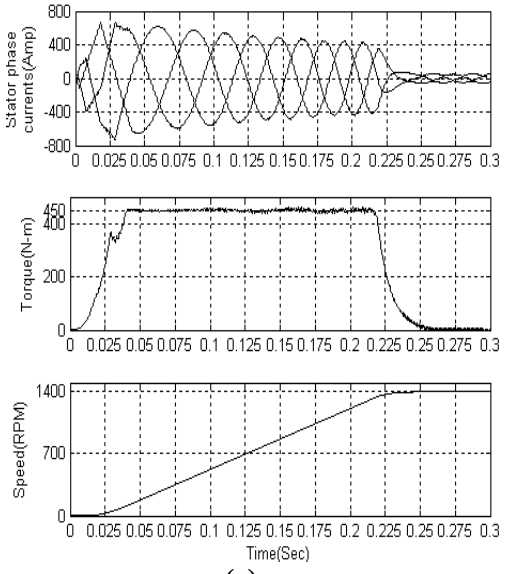

(a)

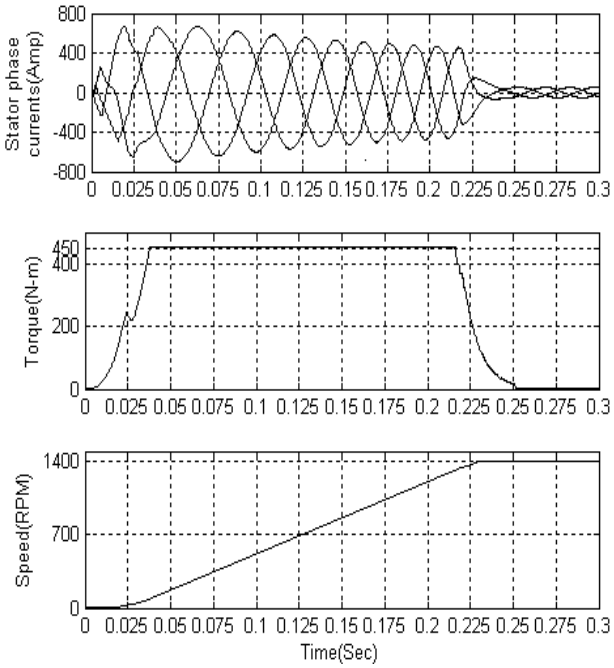

(b)

Fig. 5 Performance of Induction Motor Drive during the Starting (a) Two-Level inverter, (b) Three-Level Inverter,

The performances under steady state are shown in Figure 6(a) and (b). The torque ripple is much more with two-level compared to three-level fed induction motor drive under low switching frequency. It varies between – 15 and + 10 with a conventional two-level inverter and is significantly reduced to < 1 with three-level inverter under steady state condition. The ripple content in the current wave forms is less and there is no oscillation in the speed response with three-level fed induction motor drive. In this, the speed response is unable to attain the reference value properly; in order to attain the reference value, the inverter DC link voltage of two-level inverter should be increased, otherwise the switching frequency should be increased, which is not possible in high-power applications because switching frequency is restricted to 1 kHz.

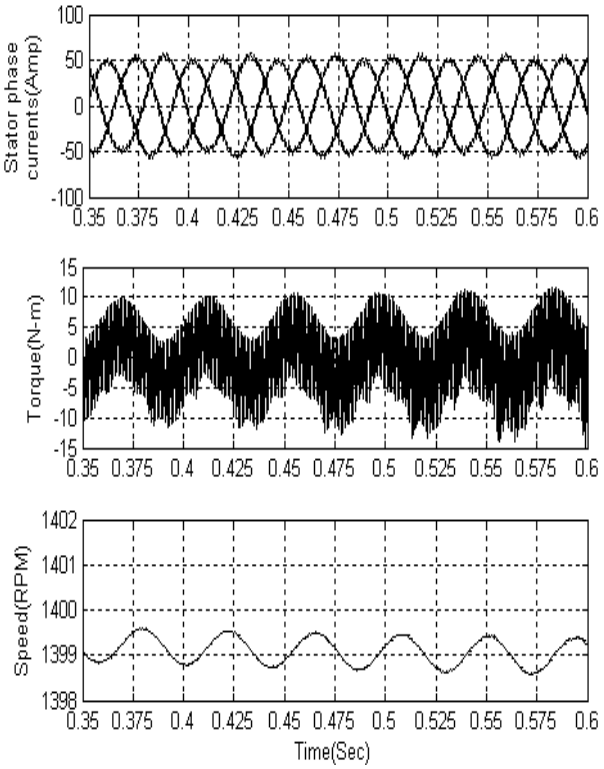

(a)

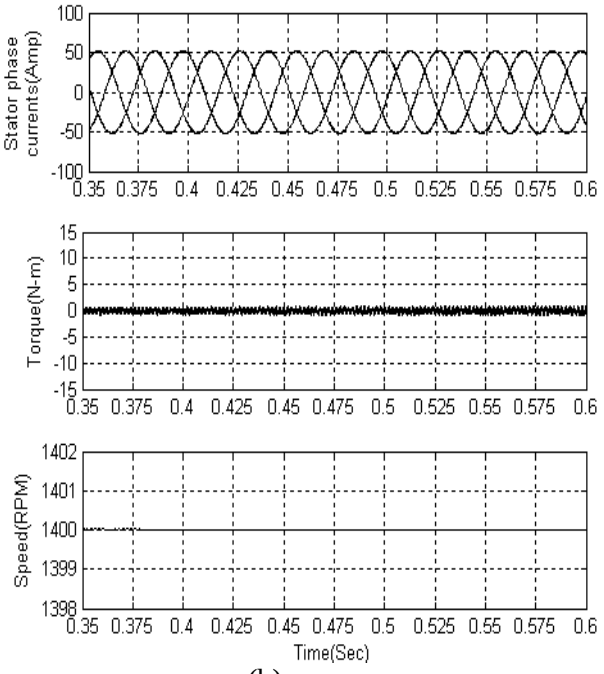

(b)

Fig. 6 Steady State Performance of Induction Motor Drive (a) Two-Level Inverter, (b) Three-Level Inverter.

The performance during step change in load torque (load torque of 100 N-m is applied at 0.6 sec and removed at 0.8 sec) is shown in Figure 7(a) and (b) respectively. Ripple content in the wave forms is less and the decrease in speed is less with the three-level fed induction motor drive.

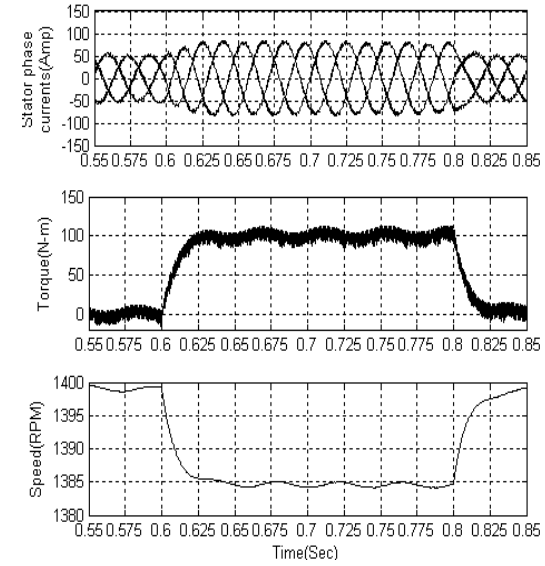

(a)

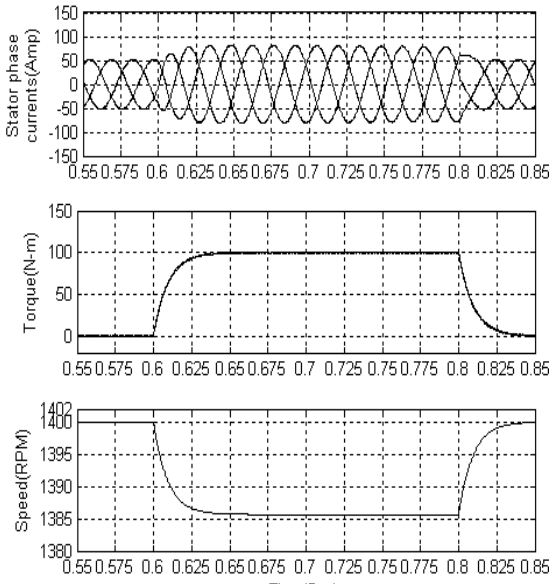

(b)

Fig. 7 Performance during Step Change in Load Torque (a) Two-Level Inverter, (b) Three-Level Inverter.

The drive performance during speed reversals (From +1200 to -1200) and (from -1200 to +1200) with two-level and three-level is shown in Figure 8(a) and (b), Figure 9(a) and (b) respectively. In this, the speed response reaches little early with three-level compared to two-level fed induction motor drive.

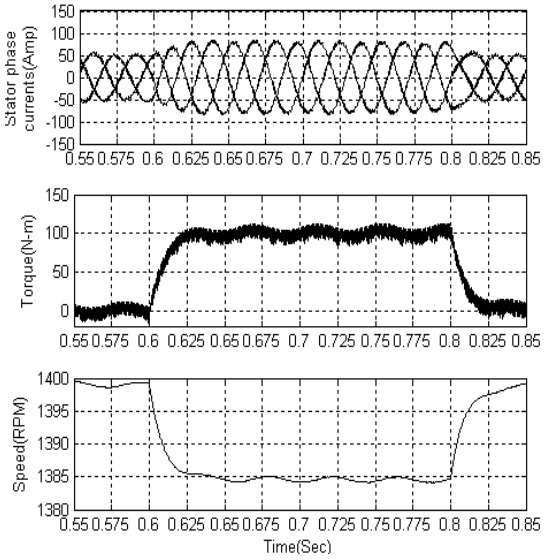

(a)

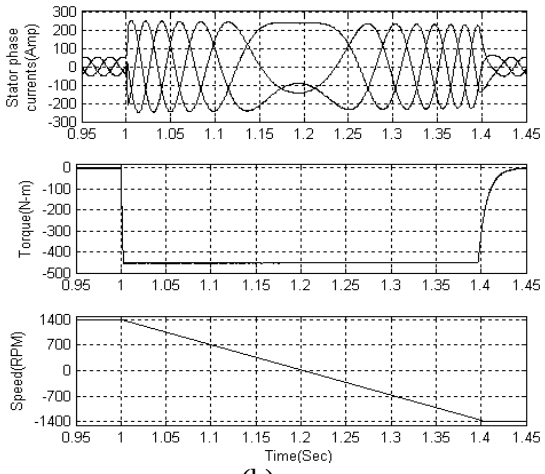

(b)

Fig. 8 Performance during Speed Reversal Operation (Speed Is Changed from + 1200 rpm to 1200 rpm) (a) Two-Level Inverter, (b) Three-Level Inverter.

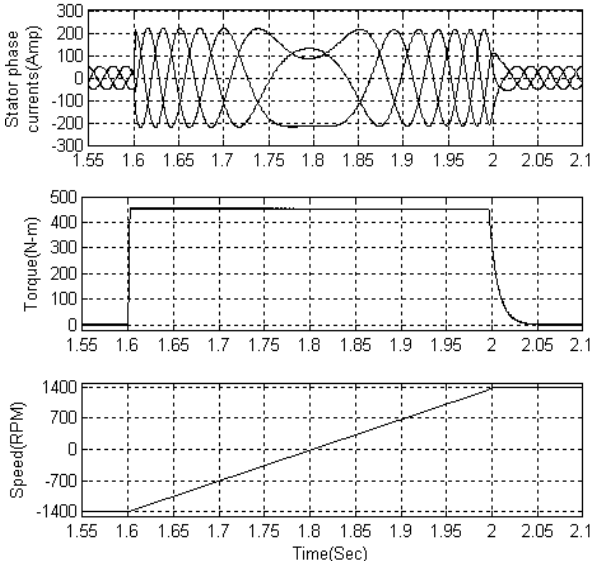

(a)

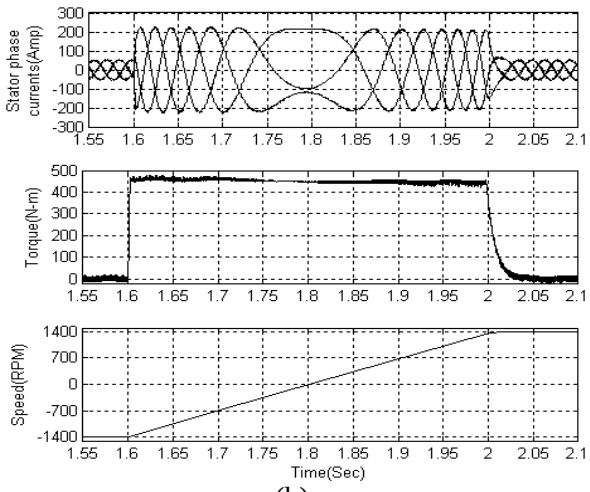

(b)

Fig. 9 Performance during Speed Reversal Operation (Speed Changed from – 1200 rpm to + 1200 rpm) (a) Two-Level Inverter (b) Three-Level Inverter.

Figure 10(a) and (b) show the torque ripple with conventional two-level and three-level fed induction motor drive under steady state condition. The torque ripple significantly reduces from the value of 13 to < 1 with three-level inverter under low switching frequency (1 kHz). It is also found that torque ripple is significantly minimized when the load torque is changed suddenly. The torque ripple during step change in load torque with two-level and three-level is given Figures 11(a) and (b) respectively. In this case also, ripple content in the wave form is reduced drastically. Due to this reduction, a smooth speed response is attained.

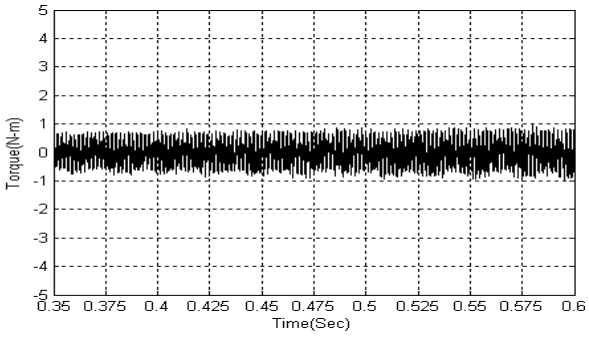

(a)

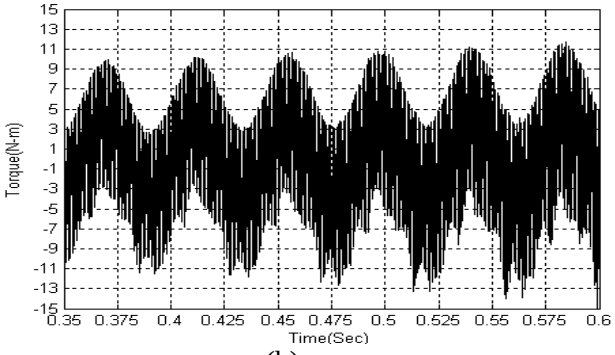

(b)

Fig. 10 Torque Ripple under Steady State (a) Two-Level, (b) Three-Level.

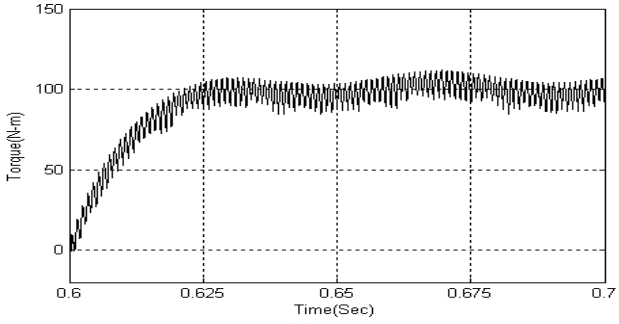

(a)

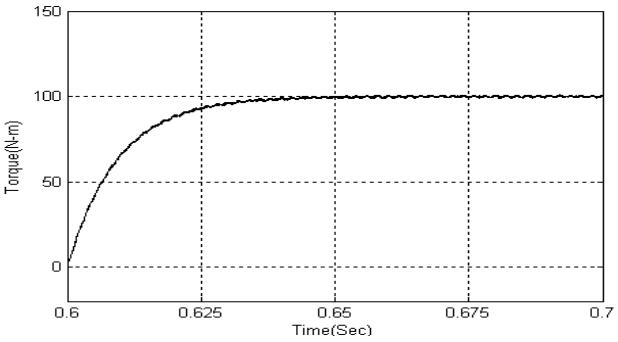

(b)

Fig. 11 Torque Ripple during Step Change in Load Torque (a) Two-Level (b) Three-Level.

Comparison THD at Various Switching Frequencies

The percent THD values of two-level and three-level inverter fed induction motor drive phase currents (i_a, i_b and i_c) under low-switching frequency (1000 Hz) is as given below in Table III.

Phase currents	%THD with two-level	%THD with three-level
ia	8.77	0.92
ib	10.73	1.34
ic	15.83	1.01

CONCLUSIONS

The performance of indirect vector-controlled induction motor drive with two-level and three-level under low switching frequency (1 kHz) is presented in this paper. It is observed that with the increase in inverter level, there is an improvement in the performance of induction motor compared to the conventional two-level inverter. The starting transients and ripple content in the current waveforms are also reduced with a three-level. The momentary speed decrease in speed is also less with three-level inverter when three is step change in the load. The torque ripple is drastically reduced by 80% and THD of phase currents decreased by 87% with three-level inverter compared to two-level inverter fed induction motor drive under low switching frequency. Besides this, the simplified SVM offers the following advantages:

1. It saves the controller memory in case of experimental realization because switching sequence is determined without look-up table.
2. It reduces the execution time because the effective times of vectors are calculated in the same manner as of two-level SVM.

APPENDIX

Three-phase, 400 V, 100 hp, 1480 rpm induction motor

Parameters:

Stator resistance Rs = 0.03552 Ω

Stator inductance Ls = 0.015435 H

Rotor resistance Rr = 0.02092 Ω

Rotor inductance Lr = 0.015435 H

Mutual inductance Lm = 0.0151 H

Moment of inertia J = 1.25 Kg-m^2

REFERENCES

1. Peter Vas. *Vector Control of AC Machines* 1990. New York. Clarendon Press.
2. Toshiaki Murata, Takeshi Tsuchiya and Ikuo Takeda. *IEEE Transactions on Industrial Electronics*. 1990. 37(4). 283–290p.
3. Chih-Yi Huang, Chao-Peng Wei, Jung-Tai Yu et al. *IEEE Transactions. on Industrial Applicaionst*. Oct. 2005. 52(5). 1364–1371p.
4. M. Masiala, B. Vafakhah, A. Knight et al. *Proceedings of IEEE CCECE*. 2007. 397–400p.
5. Dong Hwa Kim. *Applied Soft Computing*. Elsevier. Jun. 2007.
6. O.Barambones and P.Alkorta. *Asian Journal of Control*. Sep. 2010. 12(5). 640–649.
7. P.M.Bhagwat and V.R.Stefanovic. *IEEE Transactions on Industrial Applications.* Nov-Dec. 1983. IA-19. 1057–1069p.
8. G.Sinha and T.A.Lipo. *IEEE Transactions on Industrial Applications.* Jul-Aug. 1994. 30. 938–944p.
9. G.Carrara, S.Gardella, M.Marchesoni et al. *Proceedings of IEEE PESC'90*. 1990. 363–371p.
10. M.Cosan, H.Mao, D.Borojevic et al. *Proceedings of VPEC Seminar*. 1996. 123–128p.
11. H. L. Liu and G. H. Cho. *IEEE Transactions on Power Electronics.* Sept. 1994. 9. 481–486p.
12. B.Kaku, I.Miyashita and S.Sone. *Proceedings of IEE-Electrical Power Applications*. May 1997. 144(3). 182–190p.
13. N.Celanovic and D.Boroyevich. *IEEE Transactions on Power Electronics*. Mar. 2000. 15. 242–249p.
14. Jae Hyeongg Seo, Channg Ho Choi and Dong Seok Hyun. *IEEE Transactions On Power Electronics*. Jul. 2001. 16. 545–550p.
15. Wenxi Yao, Haibing Hu and Zhengyu Lu. *IEEEE Transactions on Power Electronics*. Jan. 2008. 23. 45–51.
16. Paul C. Krause, Oleg Wasyanczuk and Scott D.Sudhoff. *Analysis of Electrical Machinery and Drive Systems.* India. IEEEE Press. 2002.

AUTHOR BIOGRAPHIES

G. Durgasukumar received Bachelor's and Master's degrees in Electrical Engineering from J.N.T.U, Hyderabad (India) and is pursuing his Ph.D. degree in the Electrical Engineering Department, Indian Institute of Technology, Roorkee, India. His research interests include power electronics and electric machines and drives. He is presently pursuing Ph.D. under the guidance of M.K.Pathak.

Mukesh Kumar Pathak was born in Hamirpur (H.P.), India, in 1966. He did his graduation in Electrical Engineering from L.D. Engineering College, Ahmedabad (Gujarat), India, in 1986. He joined the Electrical Engineering Department

of NIT, Kurukshetra (Haryana), India, as a Lecturer in 1987. In 1989, he joined the Electrical Engineering Department of NIT, Hamirpur (HP), India, where he served till 2007. Presently, he is working as an Assistant Professor in the Electrical Engineering Department of IIT Roorkee, India, where he joined in 2007. He obtained both his M.Tech (Power Electronics, Electrical Machines and Drives) and Ph.D. degrees from IIT, Delhi, India. He has co-authored a book on Electric Machines. He is a member of IEEE, a life fellow of the Institution of Engineers (India), a life member of the Indian Society for Technical Education (ISTE) and Systems Society of India (SSI).